



## Brief Communication

## Origin and evolution of the kiwifruit Y chromosome

Junyang Yue<sup>1,2,\*</sup> , Qinyao Chen<sup>1,†</sup>, Sijia Zhang<sup>1,†</sup>, Yunzhi Lin<sup>1</sup>, Wangmei Ren<sup>1</sup>, Bingjie Li<sup>1</sup>, Ying Wu<sup>1</sup>, Yingzhen Wang<sup>1</sup>, Yongfeng Zhou<sup>2,\*</sup>  and Yongsheng Liu<sup>1,\*</sup><sup>1</sup>School of Horticulture, Anhui Agricultural University, Hefei, China<sup>2</sup>Agricultural Genomics Institute at Shenzhen, Chinese Academy of Agricultural Sciences, Shenzhen, Guangdong, China

Received 11 May 2023;

revised 5 September 2023;

accepted 15 October 2023.

\*Correspondence (Tel +86 551 65786185; fax +86-551-65786185; email liuyongsheng1122@ahau.edu.cn (Y.L.); Tel +86 755 23250158; fax +86-755-23250158; email zhouyongfeng@caas.cn (Y.Z.))

†These authors contributed equally.

**Keywords:** *Actinidia*, kiwifruit, Y chromosome, genome evolution, structural variation.

*Actinidia*, often known as kiwifruit, is functionally dioecious with separate female and male individuals. The sex determination of kiwifruit is genetically controlled by an XY system, even independent of ploidy levels. Recently, two Y-linked sex-determining genes, *Shy Girl* (*SyGl*) and *Friendly Boy* (*FrBy*), have been successively identified and characterized in *A. chinensis* (Akagi *et al.*, 2018; Akagi *et al.*, 2019). By coupling comparative genomic analyses, *SyGl* and *FrBy* were found to be conserved across species, indicating they arose from a common kiwifruit ancestor. Interestingly, though, their genomic locations differ among chromosomes with at least two turnover events (Akagi *et al.*, 2023), suggesting a highly modular evolutionary history after species divergence.

To explore the structural reorganization of the kiwifruit Y chromosome, we have individually *de novo* assembled two chromosome-scale haplotype-resolved male genomes of *A. chinensis* 'H0809' ( $2n = 2x = 58$ ) and *A. eriantha* 'Blank' ( $2n = 2x = 58$ ) (Table S1). Whole-genome comparisons showed a high degree of synteny between their four haplotypes and the T2T reference genome (Yue *et al.*, 2023), indicating our assembled genomes were of high quality. The availability of phased diploid sex chromosomes could directly exhibit a physically large hemizygous region, which has been ascertained as the sex-determining region (SDR) harbouring both *SyGl* and *FrBy* on each Y chromosome (Figure 1a; Figure S1). While SDR in *A. chinensis* (AchSDR) was unsurprisingly located on chromosome 25 (Chr25), SDR in *A. eriantha* (AerSDR) was identified on Chr12, revealing a novel inter-chromosomal translocation between sex chromosomes and autosomes. This large structural variation was further supported by genetic mapping in an interspecific F1 population of *A. chinensis* 'Hongyang' and *A. eriantha* 'Blank' (Figure S2).

Consistent with previous findings in *A. arguta*, *A. polygama* and *A. rufa* (Akagi *et al.*, 2023), the chromosomal collinearity between AchSDR and AerSDR was also very low. To understand this diversity, it is necessary to compare the functional genes in the two SDRs. Totally, we identified 39 and 19 protein-coding genes from AchSDR and AerSDR respectively (Figure 1b). Of these, only five orthologous genes were shared in common, encoding *SyGl*, *FrBy*, ATP synthase, FT and PSI-F. When comparing

SDRs to whole genomes, the shared genes accounted for a much smaller percentage (Table S2). The genomic rate of SDR adaptive evolution should indicate that the transition of sex chromosomes occurred long time ago but not recently.

Reflection of the evolutionary trajectories of *SyGl* and *FrBy* is the key to understanding the origin of the Y chromosome in kiwifruit. What is certain is that the ancient SDR was established before kiwifruit species divergence. In both *A. chinensis* and *A. eriantha*, *SyGl* and *FrBy* each had another paralogous member, *SyGl-like* and *FrBy-like*, locating on Chr19 and Chr10 respectively (Figure S1), which indicated that they were derived from a lineage-specific gene duplication. By calculating synonymous substitution ( $K_s$ ), the values of *SyGl* paralogs were generally smaller than the first peak value of genome-wide paralogs from *A. chinensis* and *A. eriantha*, suggesting the recent WGD event ( $x$ ) may contribute to the expansion of these sex-determining genes (Figure 1c). As *SyGl* and *FrBy* were traced back to different chromosomes (Figure S3), additional and multiple movements should be required to form the initial SDR. By searching paralogs of those genes surrounding *SyGl-like* and *FrBy-like*, the counterparts of Chr19 and Chr10 after WGD were speculated to be Chr06 and Chr07 respectively (Figure S4). Meanwhile, we found that PIF/Harbinger has played a vital role in promoting the movements of *SyGl* and *FrBy* from autosomes to the Y chromosome in kiwifruit ancestor (Table S3).

To document the parallel evolution of SDRs after species divergence, we have examined the whole genome structures of *A. chinensis* and *A. eriantha*. A large proportion of long terminal repeat retrotransposons (LTR-RTs) were observed in both of the two SDRs (Figure 1d), showing their contributions not only to the local sequence expansion of AchSDR and AerSDR, but also to the huge genomic diversity between AchSDR and AerSDR. When estimating LTR-RT insertion times, nearly all the intact LTR-RTs were inserted during the last 2 Mya, shortly after the speciation event (~3.5 Mya) of *A. chinensis* and *A. eriantha* (Figure 1e,f). Particularly, we found a new round of LTR-RT burst event occurred within the recent 0.1 Mya in both genomes, reflecting the ongoing rapid evolution driven by LTR-RTs in kiwifruit.

To elucidate the proximate mechanisms causing reduced recombination between sex chromosomes, we split each of the two SDRs into 2-kb bins and defined the rest of genome (without SDR) as sex-undetermining region (SUR). Then, cross-comparisons were performed among the four data sets of AchSDR, AerSDR, AchSUR and AerSUR. In *A. chinensis*, 625 2-kb bins from AchSDR were shared with at least another one data set (Figure S5). Of these, the vast majority (~96.5%) could be traced back to AchSUR, supporting their lineage-specific duplications. Similarly, AerSDR in *A. eriantha* had 446 conserved bins, where 93.7% were sourced from AerSUR (Figure S5). On the other hand, 100

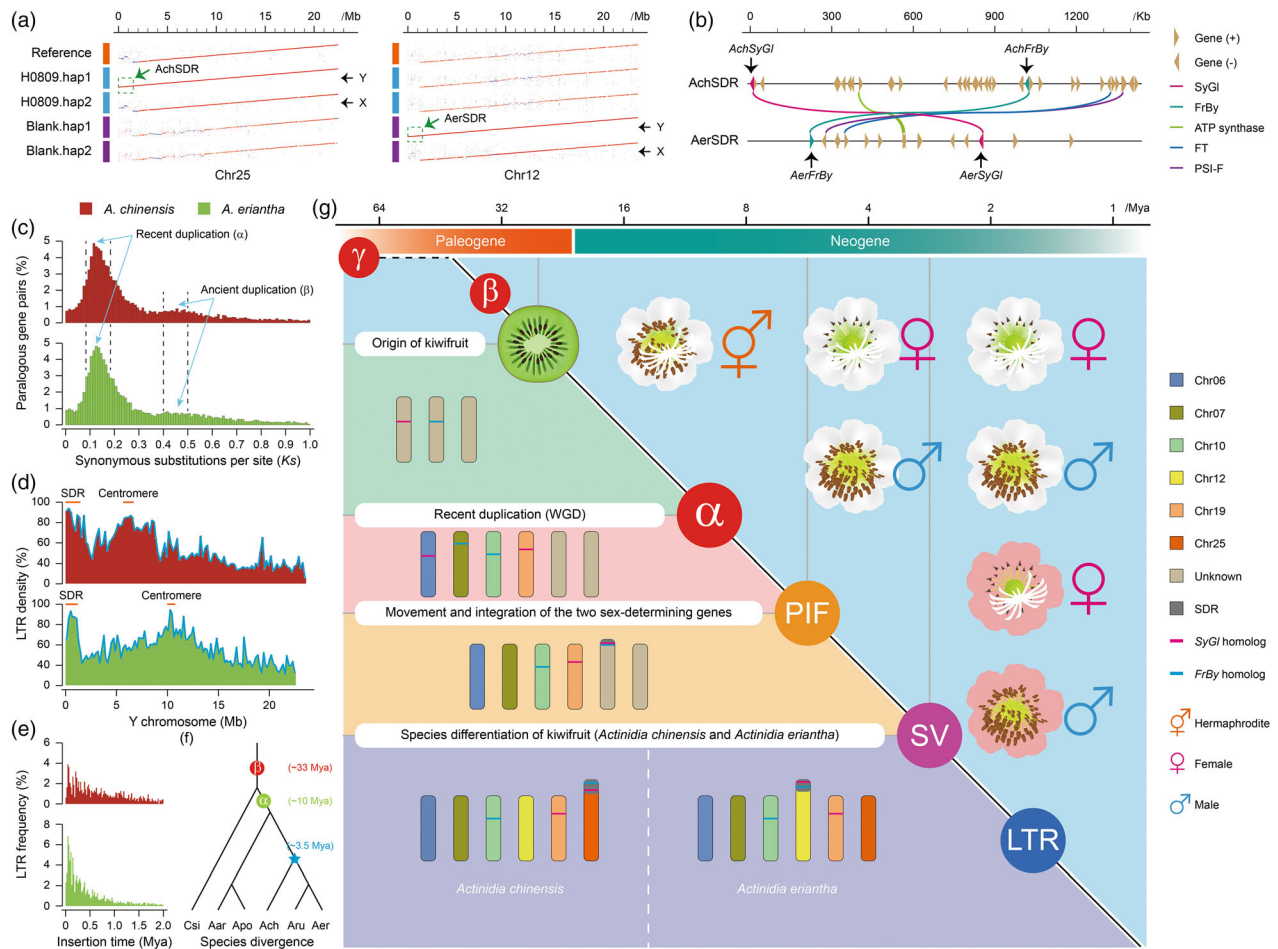


**Figure 1** A dynamic view of the Y chromosome evolution in kiwifruit. (a) Collinearity of the sex chromosome between H0809, Blank and the T2T reference genome. (b) Protein-coding genes identified from AchSDR and AerSDR. (c) WGD events in *A. chinensis* and *A. eriantha*. (d) Density of LTR-RTs across the Y chromosome in 100 kb bins. (e) Estimation of LTR-RT insertion times. (f) Schematic representation of species divergence among *A. arguta* (Aar), *A. polygama* (Apo), *A. chinensis* (Ach), *A. rufa* (Aru) and *A. eriantha* (Aer). (g) WGD events and TE activities are responsible for the emergence, development, expansion, evolution and divergence of SDRs in kiwifruit. Meanwhile, an early inter-chromosomal translocation of SDRs has directly resulted in different sex chromosomes between *A. chinensis* and *A. eriantha*.

and 151 unique bins were, respectively, obtained from AchSDR and AerSDR, reflecting the dynamics of variations in each genome. Genome-wide location analysis showed that these unique bins tend to situate at the junctions of SDRs and pseudoautosomal regions (PARs), which may have potential benefits for suppressing homologous recombination between the X and Y chromosomes in kiwifruit (Figure S6). Furthermore, centromeric localization demonstrated that recombination inhibition of SDR can be determined by itself, but not dependent on chromosome centromeres (Figure 1d), which should be an isolated case in *A. chinensis* (Pilkington *et al.*, 2018).

In summary, the formation of SDR was driven by both WGD events and TE activities that were composed of multiple rounds of DNA duplication, modification, fusion and variation from the ancestral to differentiated species of kiwifruit. Here, we present a model for better understanding of the evolutionary trajectory that underlies the emergence, expansion and divergence of the kiwifruit Y chromosome (Figure 1g).

#### Accession number

The raw reads are available at the NCBI BioProject (PRJNA957968).

#### Acknowledgements

This work was supported by the National Natural Science Foundation of China (31972474, 90717110) and Anhui Provincial Natural Science Foundation (2308085MC69).

#### Conflicts of interest

The authors declare no conflict of interest.

#### Author contributions

J.Y., Y. Liu and Y.Z. conceived the ideas and wrote the article. Y. Liu, W.R. and Y. Wang prepared the materials. J.Y., Q.C., S.Z., Y. Lin, B.L. and Y. Wu analysed the data. All authors read and approved the final article.

#### Data availability statement

The raw reads are available at the NCBI BioProject under accession number PRJNA957968.

## References

- Akagi, T., Henry, I.M., Ohtani, H., Morimoto, T., Beppu, K., Kataoka, I. and Tao, R. (2018) A Y-encoded suppressor of feminization arose via lineage-specific duplication of a cytokinin response regulator in kiwifruit. *Plant Cell*, **30**, 780–795.
- Akagi, T., Pilkington, S.M., Varkonyi-Gasic, E., Henry, I.M., Sugano, S.S., Sonoda, M., Firl, A. *et al.* (2019) Two Y-chromosome-encoded genes determine sex in kiwifruit. *Nat. Plants*, **5**, 801–809.
- Akagi, T., Varkonyi-Gasic, E., Shirasawa, K., Catanach, A., Henry, I.M., Mertten, D., Datson, P. *et al.* (2023) Recurrent neo-sex chromosome evolution in kiwifruit. *Nat. Plants*, **9**, 393–402.
- Pilkington, S.M., Crowhurst, R., Hilario, E., Nardoza, S., Fraser, L., Peng, Y., Gunaseelan, K. *et al.* (2018) A manually annotated *Actinidia chinensis* var. *chinensis* (kiwifruit) genome highlights the challenges associated with draft genomes and gene prediction in plants. *BMC Genomics*, **19**, 257.
- Yue, J., Chen, Q., Wang, Y., Zhang, L., Ye, C., Wang, X., Cao, S. *et al.* (2023) Telomere-to-telomere and gap-free reference genome assembly of the kiwifruit *Actinidia chinensis*. *Hortic. Res.* **10**, uhac264.

## Supporting information

Additional supporting information may be found online in the Supporting Information section at the end of the article.

**Figure S1** Homologous analysis of *SyGl* and *FrBy*.

**Figure S2** Genetic mapping in a hybrid F1 population.

**Figure S3** Paralogs of those genes surrounding *SyGl* and *FrBy*.

**Figure S4** Paralogs of those genes surrounding *SyGl-like* and *FrBy-like*.

**Figure S5** Statistics of unique and shared bins.

**Figure S6** Distribution of unique and shared bins.

**Appendix S1** Methods.

**Table S1** Summary statistics of the assembled genomes.

**Table S2** Summary statistics of the shared genes.

**Table S3** Summary statistics of the TE families surrounding *SyGl* and *FrBy*.